DYNAMIC BEHAVIOR OF CABLE SYSTEMS WITH SPACERS FOLLOWING ICE SHEDDING

László E. Kollár and Masoud Farzaneh
NSERC/Hydro-Québec/UQAC Industrial Chair on Atmospheric Icing of Power Network Equipment (CIGELE) and Canada Research Chair on Atmospheric Icing Engineering of Power Network (INGIVRE) at the University of Québec at Chicoutimi, 555 Boulevard de l'Université, Chicoutimi, Québec G7H 2B1, Canada (http://www.cigele.ca)

ABSTRACT: The dynamic behavior of systems of two, three and four conductors with spacers is examined in the present study. A finite element model of cable system is constructed and is used to carry out modal analysis and to simulate vibrations following ice shedding from one subconductor. The modal analysis calculates the first few natural frequencies and provides the damping performance of the system. Solutions are compared with those obtained for single bare and iced cables. The results of simulations show how the resistance of cable systems against the dynamic effects of vibrations following ice shedding increases with the application of spacers and with increasing number of subconductors in the bundle.

1. INTRODUCTION

Ice accretion on cables of overhead transmission lines is a serious and frequently arising problem in cold regions. The accreted ice leads to heavy static load, while ice shedding may result in high-amplitude vibrations which are usually associated with excessive transient dynamic forces. The types of damages which may appear due to vibrations following ice shedding are short-circuit, insulator damage, hardware breakage and tower damage. A solution for this problem is the application of spacers in conductor bundles, which had electrical reasons originally, but they also help to reduce the severity of cable vibrations. A recent survey on spacers including types, materials, design characteristics, test methods and field experience is presented in CIGRE [1].

High-amplitude cable vibrations have been studied in a vast number of publications. A numerical tool applied effectively to simulate cable motion due to ice shedding, wind effect or conductor breakage is the finite element method. Ice-shedding induced vibration of single cables was examined numerically in Jamaleddine *et al* [2], Roshan Fekr & McClure [3], Kollar & Farzaneh [4] and Kalman *et al* [5]. The models presented in these studies were constructed using the finite element analysis software ADINA [6].

The present study considers cable systems with spacers, which are applied in overhead transmission lines, and investigates their dynamic behavior. In order to achieve

this goal, a finite element model of one span of bundled conductors is constructed. Modal analysis is implemented using ADINA, and the first 18 natural frequencies together with the damping ratios are determined. Simulation results of different ice-shedding scenarios are also presented; and the main achievements are summarized in Conclusions.

2. CONSTRUCTION OF MODEL OF CABLE SYSTEM

The equations of motion of the bundle are based on the principle of virtual work, which takes the following form for the assemblage of finite elements (Bathe [7]):

$$\sum_k \int_{V^{(k)}} \bar{\boldsymbol{\varepsilon}}^{(k)T} \boldsymbol{\tau}^{(k)} \mathrm{d}V^{(k)} = \sum_k \int_{V^{(k)}} \bar{\mathbf{u}}^{(k)T} \mathbf{f}^{B(k)} \mathrm{d}V^{(k)} + \sum_k \int_{S_1^{(k)},\ldots,S_q^{(k)}} \bar{\mathbf{u}}^{S(k)T} \mathbf{f}^{S(k)} \mathrm{d}S^{(k)} + \sum_i \bar{\mathbf{u}}^{iT} \mathbf{R}_C^i \tag{1}$$

where the $\bar{\mathbf{u}}$ are the virtual displacements, $\bar{\boldsymbol{\varepsilon}}$ is the corresponding virtual strain, $\boldsymbol{\tau}$ is stress, $\mathbf{f}^B$ and $\mathbf{f}^S$ are body force and surface traction over the surface area S, $S_1^{(k)}$, …, $S_q^{(k)}$ are part of S, $\mathbf{R}_C^i$ are concentrated loads with i denoting the point of load application, and k refers to element k. The virtual displacement of element k at any point, $\bar{\mathbf{u}}^{(k)}$, is assumed to be a function of the virtual displacement at the nodal points, $\bar{\mathbf{U}}$:

$$\bar{\mathbf{u}}^{(k)}(x,y,z) = \mathbf{H}^{(k)}(x,y,z)\bar{\mathbf{U}} \tag{2}$$

where $\mathbf{H}$ is the displacement interpolation matrix, while the corresponding virtual element strain as well as the element stress are obtained as

$$\bar{\boldsymbol{\varepsilon}}^{(k)}(x,y,z) = \mathbf{B}^{(k)}(x,y,z)\bar{\mathbf{U}} \quad \text{and} \quad \boldsymbol{\tau}^{(k)} = \mathbf{E}^{(k)}\boldsymbol{\varepsilon}^{(k)} + \boldsymbol{\tau}^{I(k)} \tag{3}$$

with $\mathbf{B}$ and $\mathbf{E}$ being the strain-displacement matrix and stress-strain material matrix, respectively, and $\boldsymbol{\tau}^I$ denoting initial stress due to initial strain. Substituting Equations (2)-(3) into Equation (1), the equation of static equilibrium may be obtained:

$$\mathbf{KU} = \mathbf{R} \tag{4}$$

where $\mathbf{K}$ is the stiffness matrix:

$$\mathbf{K} = \sum_k \int_{V^{(k)}} \mathbf{B}^{(k)T} \mathbf{E}^{(k)} \mathbf{B}^{(k)} \mathrm{d}V^{(k)} \tag{5}$$

and $\mathbf{R}$ is the load vector including the effects of element body forces, element surface forces, element initial stresses, and the nodal concentrated loads. In a dynamic problem involving inertia and damping forces, the equilibrium equation is written as:

$$\mathbf{M}\ddot{\mathbf{U}} + \mathbf{C}\dot{\mathbf{U}} + \mathbf{KU} = \mathbf{R} \tag{6}$$

The mass matrix, $\mathbf{M}$, and the damping matrix, $\mathbf{C}$, are expressed as follows:

$$\mathbf{M} = \sum_k \int_{V^{(k)}} \rho^{(k)} \mathbf{H}^{(k)T} \mathbf{H}^{(k)} \mathrm{d}V^{(k)} \quad \text{and} \quad \mathbf{C} = \sum_k \int_{V^{(k)}} \kappa^{(k)} \mathbf{H}^{(k)T} \mathbf{H}^{(k)} \mathrm{d}V^{(k)} \tag{7}$$

with ρ and κ being the density and damping property parameter.

The ice-shedding phenomenon is simulated in two steps in the ADINA implementation. The static analysis determines the static equilibrium of the iced cable

system; while the dynamic analysis simulates vibrations due to ice shedding. The cable is modeled by two-node isoparametric truss elements with three translational degrees of freedom at each end, the spacers are modeled by two-dimensional beam elements, while the ice load is considered by increasing cable density (Jamaleddine *et al* [2]). Thus, the density of ice-shedding cable, ρ, is different in the static and dynamic analysis, which induces vibrations. The initial strain, ε^I, is obtained from the equilibrium of the unloaded cable in the form $\varepsilon^I = T^I/(AE)$, where T^I is the initial tension, A is cross-section, and E is Young's modulus. In what follows, the matrices **H**, **B** and **E** (and consequently **M**, **C** and **K**) will be calculated for truss and beam elements (Bathe [7]).

The spatial coordinates and the element displacements of two-node truss elements are determined by the nodal coordinates and nodal displacements, respectively

$$x_j(r) = h_1 x_j^1 + h_2 x_j^2 \quad \text{and} \quad u_j(r) = h_1 u_j^1 + h_2 u_j^2, \quad j = 1,2,3 \tag{8}$$

where $h_1 = (1-r)/2$ and $h_2 = (1+r)/2$ are interpolation functions and $r \in [-1;1]$. The only strain is the longitudinal strain in truss elements:

$$\varepsilon_{11} = \frac{\mathrm{d}x_j}{\mathrm{d}s}\frac{\mathrm{d}u_j}{\mathrm{d}s} + \frac{1}{2}\frac{\mathrm{d}u_j}{\mathrm{d}s}\frac{\mathrm{d}u_j}{\mathrm{d}s} \tag{9}$$

with s denoting arc length. The vectors of element coordinates and displacements are:

$$\mathbf{x}^T = \begin{bmatrix} x_1^1 & x_2^1 & x_3^1 & x_1^2 & x_2^2 & x_3^2 \end{bmatrix} \quad \text{and} \quad \mathbf{u}^T = \begin{bmatrix} u_1^1 & u_2^1 & u_3^1 & u_1^2 & u_2^2 & u_3^2 \end{bmatrix} \tag{10}$$

The interpolation matrix is written as $\mathbf{H} = \begin{bmatrix} h_1\mathbf{I}_3 & h_2\mathbf{I}_3 \end{bmatrix}$ with $\mathbf{I}_3$ being the 3×3 identity matrix, and then

$$\mathbf{B}_L = \left(J^{-1}\right)^2 \left(\mathbf{x}^T \mathbf{H}_{,r}^T \mathbf{H}_{,r} + \mathbf{u}^T \mathbf{H}_{,r}^T \mathbf{H}_{,r}\right) \quad \text{and} \quad \mathbf{B}_{NL} = J^{-1}\mathbf{H}_{,r} \tag{11}$$

where $\mathbf{B}_L$ and $\mathbf{B}_{NL}$ appear in the linear, $\mathbf{K}_L$, and nonlinear, $\mathbf{K}_{NL}$, stiffness matrix, respectively, and $J^{-1} = \mathrm{d}r/\mathrm{d}s$. The only nonzero stress component is S_{11}, which is a function of ε_{11}; the stress-strain relationship is therefore

$$C_{1111} = \frac{\partial S_{11}}{\partial \varepsilon_{11}} \tag{12}$$

Material properties are defined for not allowing compression and assuming Hookian small strain behavior in tension, which implies nonlinear relationship in Equation (12).

To determine the matrices in the equations describing the motion of two-dimensional beam elements, the principle of virtual work is expressed in terms of the transverse displacement, w, and the rotation of the plane originally normal to the neutral axis, θ. These parameters are determined with the nodal displacements and nodal rotations:

$$w = h_1 w_1 + h_2 w_2 \quad \text{and} \quad \theta = h_1\theta_1 + h_2\theta_2 \tag{13}$$

for two-node elements. Defining

$$\mathbf{u}^T = \begin{bmatrix} w_1 & w_2 & \theta_1 & \theta_2 \end{bmatrix} \tag{14}$$

and $J = \partial x / \partial r$, and applying the interpolation matrices $\mathbf{H}_w = \begin{bmatrix} h_1 & h_2 & 0 & 0 \end{bmatrix}$ and $\mathbf{H}_\theta = \begin{bmatrix} 0 & 0 & h_1 & h_2 \end{bmatrix}$, the matrices $\mathbf{B}_w$ and $\mathbf{B}_\theta$ may be obtained as:

$$\mathbf{B}_w = J^{-1}\begin{bmatrix} \dfrac{\partial h_1}{\partial r} & \dfrac{\partial h_2}{\partial r} & 0 & 0 \end{bmatrix} \quad \text{and} \quad \mathbf{B}_\theta = J^{-1}\begin{bmatrix} 0 & 0 & \dfrac{\partial h_1}{\partial r} & \dfrac{\partial h_2}{\partial r} \end{bmatrix} \tag{15}$$

Then the mass and stiffness matrices and the loading vector for beam elements may be determined if geometrical and material properties are known (Bathe [7]).

A 200-m-long span of an overhead transmission line with 6 m sag is considered in the model. End points are assumed to be fixed, thus, no displacement and no rotation are allowed at the corresponding nodes of cable elements near the suspension. The Bersfort ACSR 48/7 conductor is assumed in the simulations; its geometrical and material data are provided in Figure 1. Spacers are assumed to be made of aluminum and to have a height of 8 cm and width of 4 cm. The distance between bare cables of a bundle in equilibrium is 0.5 m. Four configurations are examined: single cable, twin bundle in vertical plane, triple bundle and quad bundle. Figure 1 shows the sketch of twin bundle with three spacers.

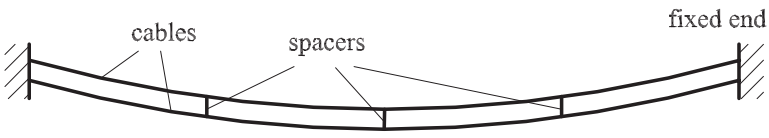

d = 35.6 mm
A = 747.1 mm^2
m_c = 2.37 kg/m
ρ = 3171 kg/m^3
E = 67.6 GPa

Figure 1: Sketch of twin bundle with three spacers including cable data (d is diameter, m_c is mass per unit length, other parameters are defined before)

3. MODAL ANALYSIS

Natural frequencies and modal damping ratios are determined in the modal analysis. The natural frequencies of a single cable are calculated from the following equations:

- $f_n = \dfrac{n}{2L}\sqrt{\dfrac{H}{m_c}}, \quad n = 1,2,3,\ldots$ in the transverse (out-of-plane) modes, (16)
- $f_n = \dfrac{n}{L}\sqrt{\dfrac{H}{m_c}}, \quad n = 1,2,3,\ldots$ in the antisymmetric in-plane modes, and (17)
- $\tan\left(\dfrac{\beta L}{2}\right) = \dfrac{\beta L}{2} - \dfrac{4}{\lambda^2}\left(\dfrac{\beta L}{2}\right)^3$ in the symmetric in-plane modes with (18)

$$\beta = 2\pi f\sqrt{\frac{m_c}{H}}, \quad \lambda^2 = \left(\frac{m_c g L}{H}\right)^2 L\frac{EA}{HL_e} \quad \text{and} \quad L_e = \int_0^L \left(\frac{\mathrm{d}s}{\mathrm{d}x}\right)^3 \mathrm{d}x$$

where f is natural frequency, L is span length, H is horizontal tension, and g is gravitational acceleration. Equations (16)-(18) may be derived by solving the boundary value problem describing the corresponding motion (Irvine & Caughey [8] and Irvine [9]). The natural frequencies of bundled conductors are determined by solving the eigenvalue problem of system (6) numerically (ADINA [6] and Bathe [7]). When investigating ice-loaded cables in the modal analysis ice load is modeled separately from the cable by two-dimensional plane-stress isobeam elements in parallel with each cable element (Kalman *et al* [5]). 50-mm-thick ice load is assumed with density of 900 $\mathrm{kg/m^3}$, Young's modulus of 10 GPa, initial yield stress of 2 MPa and Poisson's ratio of 0.33. Three spacers are installed in the span under examination, thus, the distance between adjacent spacers is 50 m.

The nth modal damping ratio is defined by the modal energy dissipation, D_n, and the modal potential energy, U_n (Yamaguchi & Nagahawatta [10]):

$$\zeta_n = \frac{D_n}{4\pi U_n} \tag{19}$$

The modal energy dissipation, D_n, may be calculated from the strain energy caused by the modal vibration, V_n, after introducing the loss factor η:

$$D_n = 2\pi\eta V_n \tag{20}$$

The modal potential energy of the cable system, U_n, is the sum of modal potential energy due to the initial cable tension, U_{tn}, and the modal strain energy, V_n:

$$U_n = U_{tn} + V_n = \int_0^L \frac{1}{2} A\sigma_0 \frac{\mathrm{d}u_j}{\mathrm{d}s}\frac{\mathrm{d}u_j}{\mathrm{d}s}\mathrm{d}s + \int_0^L \frac{1}{2} EA\varepsilon^2 \mathrm{d}s \tag{21}$$

where σ_0 is the initial stress, and ε is strain associated with modal vibration, and it is defined by Equation (9). Using Equations (19)-(21), the modal damping of a cable system consisting of l components may be expressed as follows:

$$\zeta_n = \frac{1}{2}\sum_{i=1}^{l} \eta_i \frac{V_{ni}}{U_{tn} + V_n} \tag{22}$$

4. RESULTS

4.1 Natural frequencies

Natural frequencies of the four configurations mentioned in Section 2 were calculated using ADINA. Figure 2(a) compares the first 18 natural frequencies. For a single cable the smallest natural frequency is that of the first out-of-plane mode, and then frequencies appear in pair except in mode-6 to mode-8. One of the two frequencies in each pair

corresponds to an in-plane mode, while the other one corresponds to an out-of-plane mode. The natural frequencies of the single iced cable are slightly lower than those of the bare one, which is mainly explained by the fact that the mass per unit length increases to a greater extent than the cable tension as ice load is considered on the cable. For bundled conductors several nearly equal frequencies appear in higher modes. Yamaguchi *et al* [11] presented natural frequencies of a cable system with two main cables and a secondary cable, all of which individually had similar natural frequencies, thus, they observed groups of three closely spaced frequencies. The case of bundled conductors, however, is different due to the spacers. The number of closely spaced frequencies is changeable; furthermore, complicated shapes occur in higher modes.

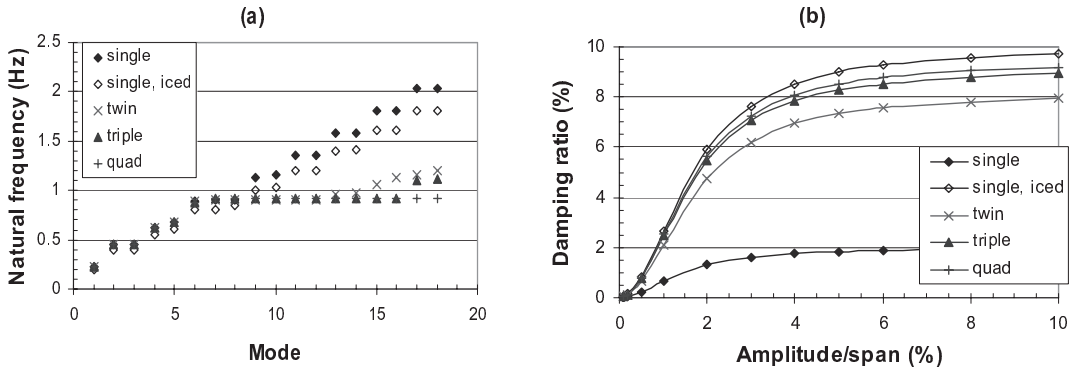

Figure 2: (a) natural frequencies (b) damping ratios of first out-of-plane mode

4.2 Modal damping ratios

The modal damping ratios of the first out-of-plane mode and the first in-plane mode were determined as a function of vibration amplitude. Figure 2(b) shows damping ratios of the first out-of-plane mode for single bare and iced cables as well as for iced bundled conductors with one bare subconductor. The loss factor was chosen to be equal to 0.04 and 0.2 for bare cable and for iced cable, respectively. The asymptotes at 2% and 10% represent the corresponding maximum value of damping, which were the proposed values of damping constants in Roshan Fekr & McClure [3]. The damping ratio of bundled conductors increases to a low extent with the number of subconductors in the bundle, and tends to that of a single iced cable, because only one bare cable is assumed in each bundle, while all the other cables are iced. This tendency is more observable for the first out-of-plane mode than for the first in-plane mode. The influence of damping ratio of spacers is negligible, since spacers store much less energy than the cables. After ice shedding, however, the higher damping ratio is not the only reason for the lower-amplitude vibration of bundles with greater number of subconductors (see Section 4.3). When ice sheds from one subconductor, the same amount of energy is distributed, which causes less severe vibration in a more complex cable system.

4.3 Results of ice-shedding simulations

Several ice-shedding scenarios were simulated with different ice thickness and with different distances between adjacent spacers. Ice thickness was varied between 10 and 60 mm, and Figure 3(a) compares the maximum jump heights of the ice-shedding cable above its unloaded position for different configurations. The jump height decreases to a great degree as a second cable is connected to the ice-shedding one. Further increase in the number of cables in the bundle decreases jump height to a significantly less extent, the difference between results obtained for triple and quad bundle is almost negligible.

The maximum jump height as a function of distance between adjacent spacers is drawn in Figure 3(b). This distance varies between 33 m and 100 m, i.e. the number of spacers changes between 5 and 1, respectively. Again, jump height decreases with increasing number of subconductors in the bundle, but the difference between results obtained for triple and quad bundle is negligible. More detailed discussion of the vibration of bundled conductors after ice shedding is provided in Kollar & Farzaneh [12].

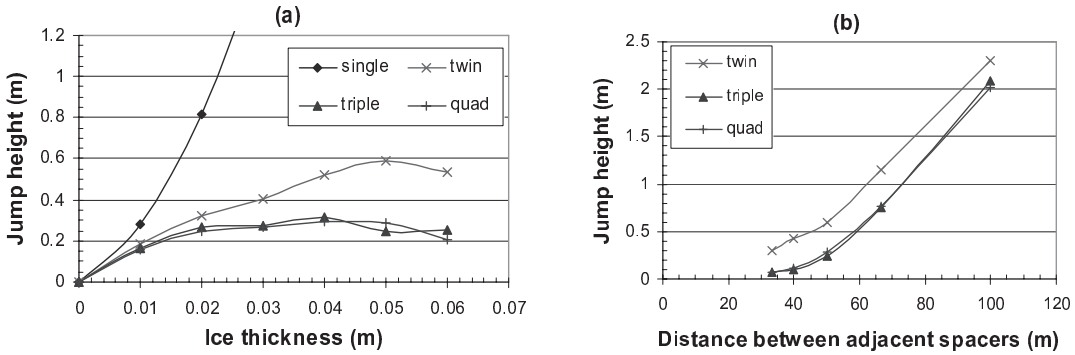

Figure 3: Jump height of ice-shedding cable above unloaded position: (a) distance between adjacent spacers is 50 m, (b) ice thickness is 50 mm

5. CONCLUSIONS

Dynamics of bundled conductors has been studied in this paper. A finite element model was constructed and applied to calculate the natural frequencies and modal damping ratios as well as to simulate vibrations following ice shedding. Groups of closely spaced natural frequencies occur in higher modes as the number of subconductors in the bundle increases. The number of nearly equal frequencies in these groups is changeable, contrarily to the case of cable systems with two main cables and a secondary cable, which was examined in a former publication (Yamaguchi *et al* [11]). Also, the damping ratio does not increase significantly due to the application of spacers, which facts are explained by the difference between the effects of spacers and secondary cables. The vibration of the ice-shedding cable, however, becomes less severe in a conductor bundle, because the same amount of energy is dissipated in a more complex cable system.

ACKNOWLEDGMENT

This research was carried out within the framework of the NSERC/Hydro-Québec Industrial Chair on Atmospheric Icing of Power Network Equipment (CIGELE) and the Canada Research Chair on Atmospheric Icing Engineering of Power Network (INGIVRE) at the University of Québec at Chicoutimi. The authors would like to thank all the sponsors of the CIGELE for their support.

REFERENCES

1. CIGRE SCB2 WG11, State of the Art Survey on Spacers and Spacer Dampers, Electra No. 277, August 2005.

2. Jamaleddine, A., McClure, G., Rousselet, J., Beauchemin, R., Simulation of Ice Shedding on Electrical Transmission Lines Using ADINA, *Computers & Structures,* 47(4/5), (1993), pp 523-536.

3. Roshan Fekr, M., McClure, G., Numerical modelling of the dynamic response of ice shedding on electrical transmission lines, *Atmospheric Research,* 46, (1998), pp 1-11.

4. Kollar, L.E., Farzaneh, M., Dynamic Analysis of Overhead Cable Vibrations as a Result of Ice Shedding, *Proceedings of 6th International Symposium on Cable Dynamics*, Charleston, SC, USA, 2005.

5. Kalman, T., McClure, G., Farzaneh M., Kollar, L.E., Leblond, A., Dynamic Behavior of Iced Overhead Cables Subjected to Mechanical Shocks, *Proceedings of the 6th International Symposium on Cable Dynamics*, Charleston, SC, USA, 2005.

6. ADINA R & D. ADINA – Theory and Modeling Guide, Watertown, MA, USA, (2003), Report ARD 03-7.

7. Bathe, K-J., *Finite Element Procedures*, Prentice Hall, Upper Saddle River, New Jersey, 1996.

8. Irvine, H.M., Caughey, T.K., The linear theory of free vibrations of a suspended cable, *Proceedings of the Royal Society of London* A, Vol. 341, (1974), pp. 299-315.

9. Irvine, H.M., *Cable Structures*, MIT Press, Cambridge, Massachusetts, 1981.

10. Yamaguchi, H., Nagahawatta, H.D., Damping effects of cable cross ties in cable-stayed bridges, *Journal of Wind Engineering and Industrial Aerodynamics*, Vol. 54/55, (1995), pp 35-43.

11. Yamaguchi, H., Alauddin, Md., Poovarodom, N., Dynamic characteristics and vibration control of a cable system with substructural interactions, *Engineering Structures,* Vol. 23, (2001), pp. 1348-1358.

12. Kollar, L.E., Farzaneh, M., Numerical Modeling of the Dynamic Response of Bundled Conductors due to Ice Shedding, submitted to *Computers & Structures*, 2006.